Structure, Vol. 13, 1881–1886, December, 2005, ©2005 Elsevier Ltd All rights reserved. DOI 10.1016/j.str.2005.09.021

Structure of Calmodulin Bound to the Hydrophobic IQ Domain of the Cardiac $Ca_V1.2$ Calcium Channel

Jennifer L. Fallon,[1] D. Brent Halling,[2]
Susan L. Hamilton,[2] and Florante A. Quiocho[1,*]
[1]Verna and Marrs McLean Department of Biochemistry and Molecular Biology
[2]Department of Molecular Physiology and Biophysics
Baylor College of Medicine
Houston, Texas 77030

Summary

Ca^{2+}-dependent inactivation (CDI) and facilitation (CDF) of the $Ca_V1.2$ Ca^{2+} channel require calmodulin binding to a putative IQ motif in the carboxy-terminal tail of the pore-forming subunit. We present the 1.45 Å crystal structure of Ca^{2+}-calmodulin bound to a 21 residue peptide corresponding to the IQ domain of $Ca_V1.2$. This structure shows that parallel binding of calmodulin to the IQ domain is governed by hydrophobic interactions. Mutations of residues I1672 and Q1673 in the peptide to alanines, which abolish CDI but not CDF in the channel, do not greatly alter the structure. Both lobes of Ca^{2+}-saturated CaM bind to the IQ peptide but isoleucine 1672, thought to form an intramolecular interaction that drives CDI, is buried. These findings suggest that this structure could represent the conformation that calmodulin assumes in CDF.

Introduction

Ca^{2+} entering through the $Ca_V1.2$ channel in cardiac myocytes triggers Ca^{2+} release from the sarcoplasmic reticulum, initiating muscle contraction (Lehmann-Horn and Jurkat-Rott, 1999; Lipscombe et al., 2004). The entering Ca^{2+} also activates a number of other Ca^{2+}-dependent enzymes and signal transduction pathways (Lehmann-Horn and Jurkat-Rott, 1999; Lipscombe et al., 2004). Alterations in channel activity can alter the action potentials of cardiac myocytes, underscoring the importance of $Ca_V1.2$ channel regulation (Alseikhan et al., 2002). Ca^{2+} entering through the channel can produce Ca^{2+}-dependent inactivation (CDI) (Dascal et al., 1986; Imredy and Yue, 1994), while a train of depolarizations of the membrane or a rise in basal Ca^{2+} levels can facilitate channel opening (Bourinet et al., 1994; Lim et al., 1990; Zühlke et al., 1999), a process designated as Ca^{2+}-dependent facilitation (CDF). Both CDF and CDI require Ca^{2+}-calmodulin (Ca^{2+}-CaM) binding to the C-terminal tail (Zühlke et al., 1999, 2000). CDI, however, requires Ca^{2+} binding only to the carboxy-terminal lobe of CaM (Peterson et al., 1999). A putative IQ motif in the carboxy-terminal tail of the α_1 subunit of $Ca_V1.2$ is critically involved in both CDI and CDF.

CaM binds Ca^{2+} ions via four EF hand loops: two at the amino-terminal or N domain, and two at the carboxy-terminal or C domain (Babu et al., 1985; for a recent review, see Bhattacharya et al. [2004]). These domains are connected by a flexible central helix. Upon binding Ca^{2+}, hydrophobic pockets (one in each domain) are exposed that enable CaM to regulate a plethora of targets. The $Ca_V1.2$ Ca^{2+}-CaM binding requires the IQ motif (amino acids 1672–1685), but other sequences (designated A and C, representing amino acids 1609–1628 and 1627–1652, respectively) have also been implicated (Erickson et al., 2003; Kim et al., 2004; Pate et al., 2000; Pitt et al., 2001; Romanin et al., 2000; Tang et al., 2003). Since $Ca_V1.2$ appears to bind only one CaM molecule (Mori et al., 2004), these different sequences are likely to contribute to a single CaM binding site, but the actual determinants of the binding are likely to be dependent on both the functional state of the channel and number of Ca^{2+} ions bound to CaM. Furthermore, the mobility of the carboxy terminus of $Ca_V1.2$ may allow interactions with other regions of the channel, or even other cytosolic components (Kobrinsky et al., 2005).

Mutagenesis studies on the channel show that alanine substitutions at isoleucine and glutamine residues (I1672 and Q1673, or simply IQ) abolish CDI and unmask CDF, while mutation of the isoleucine to glutamine destroy both CDI and CDF (Zühlke et al., 1999, 2000). The alanine mutations do not appear to inhibit Ca^{2+}-CaM binding to the C-terminal tail, as evidenced by the continued requirement for CaM to attain CDF (Zühlke et al., 1999, 2000). In contrast, the replacement of the I with E apparently also destroys CaM binding (Zühlke et al., 1999, 2000).

Kim et al. (2004) suggested that the isoleucine residue of the IQ motif is involved in linking the Ca^{2+} sensor to the downstream inactivation machinery via an interaction with the upstream EF hand motif. The EF hand motif, when bound to the Ca^{2+}-loaded Ca^{2+} sensor, was proposed to interact with a sequence in the linker between transmembrane domains one and two, allowing this I-II linker to occlude the pore. Alternatively, Anderson and coworkers suggested that the IQ sequence could bind to β subunit of the channel (Zhang et al., 2005).

As a first step to understanding the molecular mechanism by which Ca^{2+}-CaM interacts with the $Ca_V1.2$ channel and regulates both CDI and CDF, we determined the crystal structures of the Ca^{2+}-CaM bound to the CaM binding domain of $Ca_V1.2$, ^{1665}KFYATFLIQEYFRKFKKR KEQ^{1685} (hereafter referred to as "IQ peptide"), and to the same peptide with the I1672–Q1673 residues changed to alanines, a change that, in the channel, abolishes CDI but not CDF. Binding studies with these peptides demonstrate an apparent dissociation constant of ~50 nM (Black et al., 2005; Zühlke et al., 2000), with no significant change caused by the replacement of I1672–Q1673 with alanines (Tang et al., 2002). The structure obtained shows that CaM binds to this peptide in a parallel fashion, and the lack of an effect of the IQ to AA substitution suggests that the structure obtained could represent that of CaM during CDF. Movement of one of the lobes of CaM to engage other sequences that have been suggested to contribute to the CaM binding site may allow CaM to also regulate CDI.

*Correspondence: faq@bcm.tmc.edu

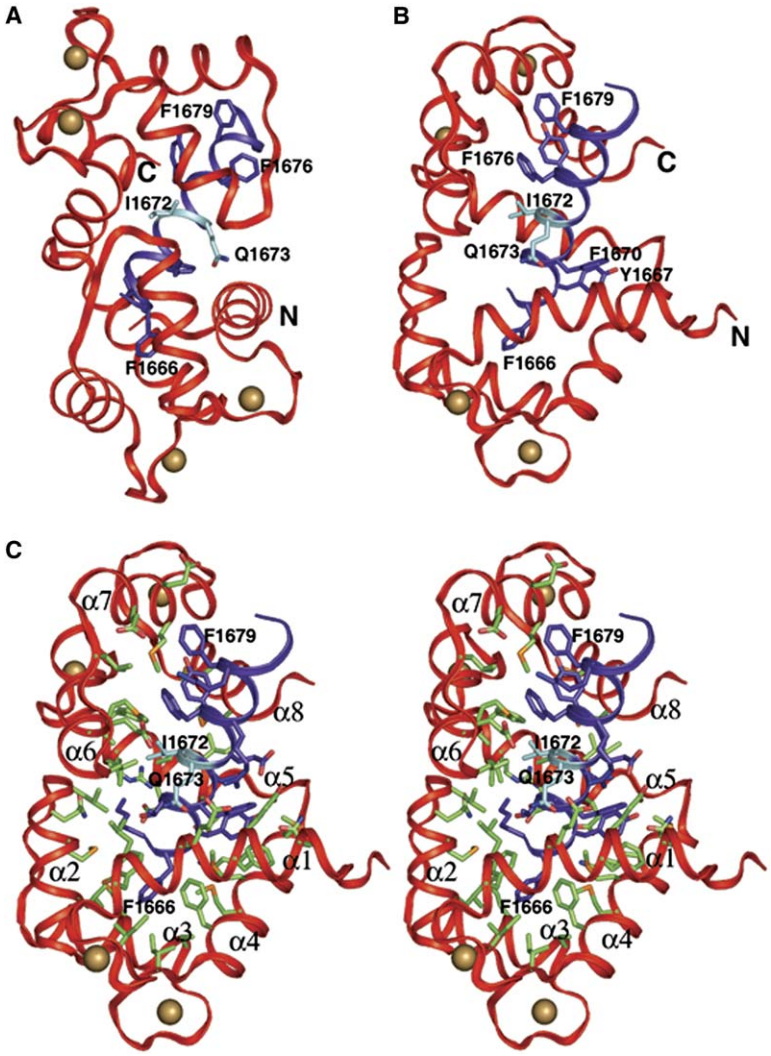

Figure 1. Views of the Structure of Ca^{2+}-CaM Bound to the IQ Peptide of the $Ca_v1.2$ Channel

(A and B) Ribbon diagram views about a 90° vertical rotation axis, with peptide I and Q residues (aqua), along with peptide aromatic residues (blue) shown. The N domain or lobe (red) of Ca^{2+}-CaM is at the bottom and the C domain or lobe is at the top. The gold spheres represent Ca^{2+}. The IQ peptide (blue) is in a nearly vertical orientation with its amino and carboxy termini at the bottom and the top, respectively.

(C) Stereoview of the structure of Ca^{2+}-CaM bound to the IQ peptide of the $Ca_v1.2$ channel. The residues (green) of CaM that are making contacts (<4.5 Å distance) with the residues of the peptide are shown. Ca^{2+}-CaM helices are labeled, along with selected peptide residues. The last residue (Q1685) of the peptide is disordered, and the side chains of K1678, K1681, R1682, K1683, and E1684 are disordered.

Results

Mode of Binding of the IQ Peptide to Ca^{2+}-CaM

In the IQ peptide bound crystal structure, Ca^{2+}-CaM is wrapped around the helical peptide in the manner previously observed for kinase-type targets (Meador et al., 1992, 1993), except that the peptide is bound in the reverse direction from that seen in compact Ca^{2+}-CaM-target peptide complex structures. Another exception to the antiparallel orientation is Ca^{2+}-CaM bound to the Ca^{2+}-CaM-dependent kinase kinase (CaMKK) peptide (Osawa et al., 1999). The pseudo 2-fold symmetry between the N and C domains of Ca^{2+}-CaM seen in the crystal structures of the bound kinase target peptides (Meador et al., 1992, 1993) is also less pronounced. The IQ peptide used in this study does not obviously conform to any other known CaM binding motif in terms of hydrophobic spacing. As can be seen in Figures 1 and 2, beginning with the N terminus of the target, the only large hydrophobic residue nestled in the hydrophobic pocket of the Ca^{2+}-CaM N domain is F1666, and this residue is apparently the beginning of the IQ peptide calmodulin binding motif. The next residue is also an aromatic residue, Y1667, which points downwards into the linker helix bend of Ca^{2+}-CaM (Figures 1 and 2). F1670 and L1671 are one turn closer to the C terminus of the peptide, in close proximity to Y1667 and the linker, with F1670 facing the N domain of Ca^{2+}-CaM and L1671 close to the C domain. This grouping of large hydrophobic target residues proximal to the CaM linker bend is unprecedented in known calmodulin-target complexes. The next two residues are the IQs (I1672 and Q1673), with I1672 contacting V91 and F92 of α5 and M109 and L112 of α6 of the C domain (Figure 1), and Q1673 participating in a hydrogen bonding network with R1677 of the IQ peptide (Figure 1) and the Ca^{2+}-CaM N-terminal (α1) helix directly and through a water molecule. E1674 makes salt links with R1677 and a carboxy-carboxylate hydrogen bond with the α6 E11 of the N domain (Figure 1).

At the C-terminal end of the IQ peptide is another cluster of aromatic residues, consisting of Y1675, F1676, and F1679 one turn down the helix (Figure 1). As can be seen in Figures 1 and 2C, all three of these aromatic residues interact with the C domain of Ca^{2+}-CaM, complicating any attempt to describe this target motif in terms of hydrophobic spacing, and demonstrating that the IQ peptide target does not closely resemble other known hydrophobic CaM binding peptide motifs.

Based on the IQ peptide sequence (see above), it might be predicted that the group of basic residues at

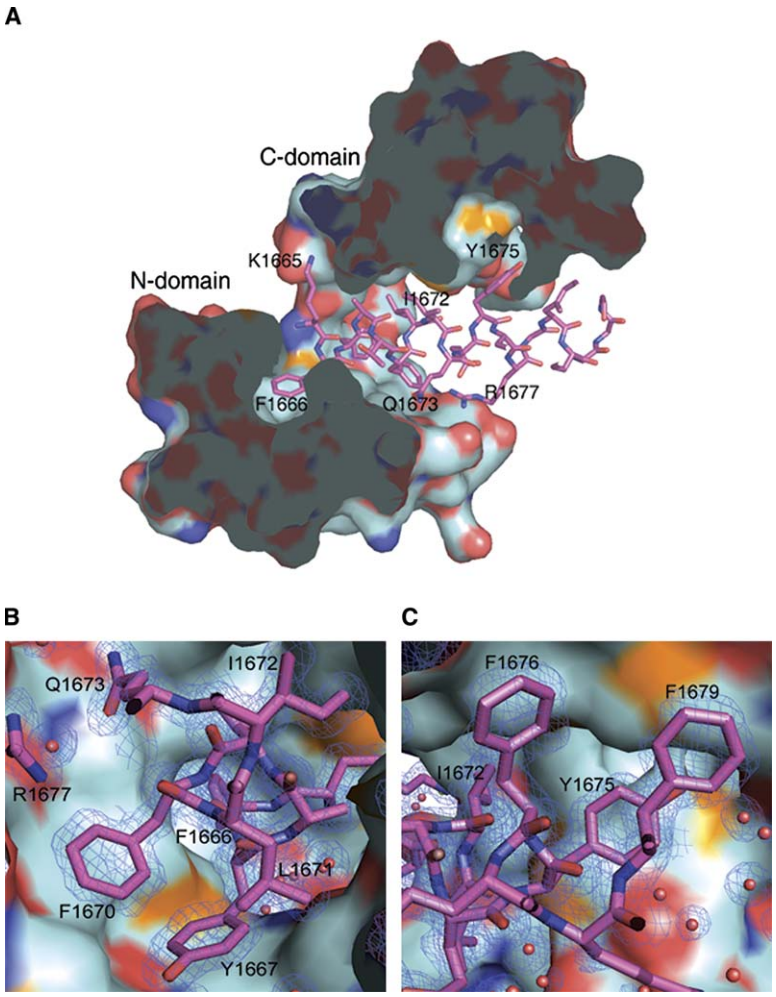

Figure 2. Views of Key Residues of the Bound IQ Peptide with CaM Surfaces

The residues of the peptide are in magenta, electron density is blue. Protein surface representations are: dark blue, +; red, −; cyan, neutral or nonpolar; and yellow, sulfur of methionine residues.

(A) Cutaway view of the complex. CaM domains are labeled, along with selected peptide residues. The N-terminal pocket of Ca^{2+}-CaM (containing F1666 of the peptide) is to the left of center. Some residues at the C-terminal end of the peptide extend above the plane of the figure and are not shown.

(B) The N-terminal hydrophobic cluster of the IQ peptide. F1666 (center background) occupies the N-terminal hydrophobic pocket of Ca^{2+}CaM. The surface is the CaM binding channel, with the N domain of Ca^{2+}-CaM to the left and the C domain to the right. F1670, Y1667, and L1671 are grouped near a nonpolar surface created by the Ca^{2+}-CaM linker (lower foreground). This hydrophobic surface is created by M71, M72, M76, and the hydrophobic portion of the K75-E84 salt link.

(C) The C-terminal hydrophobic cluster of the IQ peptide. The surface is the C-terminal hydrophobic pocket of Ca^{2+}-CaM.

the C-terminal end would be the primary determinants of the orientation of the peptide, since such clusters of positively charged residues are often found at the N-terminal region of antiparallel-oriented calmodulin targets (i.e., the N- and C-terminal portions of the target contact the C and N domains, respectively, of Ca^{2+}-CaM). However, the structure of the Ca^{2+}-CaM bound to the IQ peptide reveals a paucity of actual polar interactions with CaM. Although the highly conserved R1677 does make salt links with two glutamates of the α1 helix of the N domain and one with the peptide (E1674) (Figure 1), K1678, K1681, R1682, and K1683 do not appear to be interacting with calmodulin as they have disordered side chain electron density, while K1680 salt links to a neighboring molecule.

Domain-Domain Interactions and Linker Conformation

The domain-domain contacts in calmodulin are also unusually scarce, consisting of van der Waals interactions between α6 L112 of the Ca^{2+}-CaM C domain and α1 L18 and α2 L39 of the N domain as the principle hydrophobic contacts (Figure 1). Polar interactions in this same area are hydrogen bonds of the main chain carbonyl oxygen of α2 S38 with the side chain of N111 and H107 through a water molecule, and also a hydrogen bond from the main chain carbonyl oxygen of L39 to the side chain of K94 (data not shown). A final hydrogen bond exists between the carbonyl oxygen of Q41 through a water molecule to the side chain of R90. In the linker bend region, there is a salt link between the side chains of K75 and E84.

The linker bend in this structure is unusual in that it is a sharp type I reverse turn (Figure 1) involving exactly the same residues (D78, T79, D80, and S81) in the bend found previously only in the native ligand-free compact Ca^{2+}-CaM (Fallon and Quiocho, 2003). This turn is stabilized in the classical manner, with a 3.07 Å hydrogen bond between the main chain carbonyl oxygen of D78 and the peptide nitrogen of S81. In view of the large number of bulky hydrophobic residues in the IQ peptide target, this sharp linker bend was surprising, as a more unwound linker is usually present in Ca^{2+}-CaM-target structures (Meador et al., 1993, 1995).

In order to determine if altered CaM binding or an altered CaM conformation is responsible for the change in $Ca_V1.2$ channel inactivation seen for the 1672–1673 IQ-AA mutant (Zühlke et al., 1999, 2000), the structure of a complex with a peptide corresponding to this mutant was determined. An overlap of this structure with the Ca^{2+}-CaM-IQ target complex (Figure 3) shows no substantial changes in overall CaM conformation. The

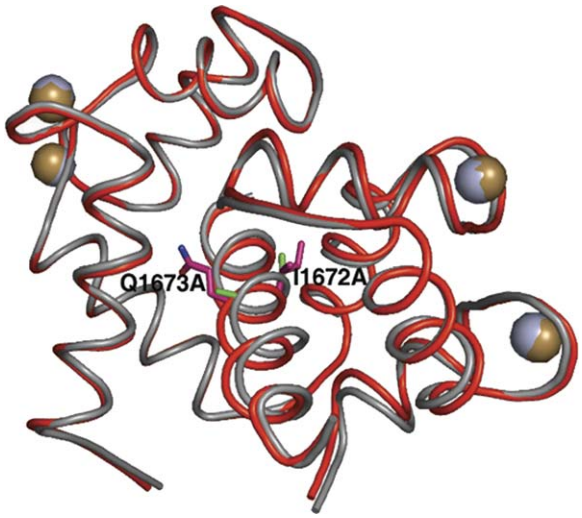

Figure 3. Overlap of the Ribbon Backbone Traces of the Structures of Complexes of Ca^{2+}-CaM with the Native IQ Peptide and the Peptide with the IQ Residues (Magenta) Replaced by Alanine (Green)

The complex with native peptide is colored red, while that with mutant peptide is gray-blue. The overall rmsd between the structures is 0.77 Å, reflected in the small relative positional displacements between the peptides and between the loop connecting the two EF hands in the C domain.

mutant peptide is slightly curved and closer to the C domain as a result of slight shifts of the peptide and the loop connecting the two EF hands in the C domain toward each other (Figure 3). A close examination of side chain conformations near the mutated region further shows some changes, most of which appear to be steric rearrangements allowed by the much smaller alanine side chains of the mutant to achieve close packing. Specifically, F92 of calmodulin makes a closer approach to the A1672 side chain, and Y1675 of the target makes a closer approach to the C domain of calmodulin. There is also a 90º rotation of the ring of Y1675 and displacement of the calmodulin methionines M144 and M145. On the opposite side of the target, the Q1673A mutation displays a water molecule in place of the polar end of the glutamine side chain, along with a slightly altered conformation of R1677. The linker bend region retains the tight type I reverse turn, with slight alterations of the ϕ-ψ angles of T79 and D80, which are reflected in the modestly different calmodulin domain orientations seen in the overlap.

Discussion

Several new features of the interaction of Ca^{2+}-CaM with the IQ peptide have emerged from the crystal structures of the complexes presented here. Perhaps the most intriguing is the parallel orientation of CaM in complex with the IQ peptide, which is reverse to that seen in all but the CaM-CaMKK complex structure (Osawa et al., 1999). The usual antiparallel orientation of the peptide seen in previous crystal structures was attributed to the influence of positively charged residues at the N-terminal end of the peptide interacting with surface aspartic and glutamic acid residues in the C domain of CaM, thereby guiding the N terminus of the peptide to bind the C domain of CaM (Meador et al., 1992, 1993) (reviewed by Bhattacharya et al. [2004]). A similar argument was used to explain the parallel orientation in the NMR structure of the Ca^{2+}-CaM bound to the CaMKK peptide and involving the basic residues at the C terminus (Osawa et al., 1999). Although there is a cluster of basic residues located at the C terminus of the IQ peptide, there are too few polar interactions in our structures to account for the parallel interaction. If the charge-coupling interactions cannot account for the reversal, then the answer must lie with the nonpolar interactions that are the vast majority of the contacts. Thus, this structure represents a unusual type of CaM binding domain recognition.

Other unusual CaM binding motifs have also been determined, including CaM in complex with the anthrax edema factor (Drum et al., 2002) and the SK potassium channel (Schumacher et al., 2001). Neither of these complexes, however, resembles the unusual structure of CaM in complex with the IQ motif. When in complex with the anthrax edema factor exotoxin, CaM is in an extended conformation and no calcium ions are bound to the N-terminal lobe of CaM in this complex. The C lobe in this complex is, however, similar to many other Ca^{2+} bound CaM C-domain structures. CaM in complex with the SK channel, however, does not have calcium bound to the C lobe of CaM. Also, in this complex, part of the linker helix of CaM is unwound to allow the cross-linking of adjacent channels by two molecules of CaM. In contrast, CaM is not in an extended conformation in complex with IQ and does have Ca^{2+} bound at both lobes.

Inspection of the hydrophobic residues of the IQ peptide target in complex with Ca^{2+}-CaM has revealed several unusual features, including the clustering in space of large hydrophobic residues, and the orientation of the N-terminal cluster toward the linker bend (Figure 2A). This last observation may explain not only the parallel orientation of the IQ target, but also the sharpness of the linker bend. If Ca^{2+}-CaM were in antiparallel orientation with respect to the IQ peptide, the linker would traverse close to the C-terminal end of the target, and the N-terminal hydrophobic cluster would be exposed to solvent. In addition, if a more unwound linker were present, the N-terminal hydrophobic cluster would again be exposed to solvent. Thus the orientation of the peptide and the sharpness of the bend are best explained by the shielding from solvent of a maximum amount of hydrophobic surface area of the IQ helical peptide, dictated by the linker-facing hydrophobic cluster. These findings, however, must be viewed with caution, as other sequences within the CaM binding region on the intact channel might interact with CaM in complex with the IQ peptide in such as way as to prevent this solvent shielding effect.

Another observation is that conversion of the isoleucine and glutamine residues at positions 1672 and 1673 to alanines, changes that, in the channel, are associated with the loss of CDI (Zühlke et al., 1999, 2000), produce only minor changes in the structure of the complex. Whether these small localized changes in the conformation of the Ca^{2+}-CaM bound to the peptide would be sufficient to account for the loss of CDI seems unlikely, but cannot be completely ruled out. One interpretation of these findings is that both structures shown here

Table 1. Data Collection and Refinement Statistics

Data Collection[a]					
			Lead MAD		
	+ Native Peptide	+ Mutant Peptide	Edge	Peak	Remote
Wavelength (Å)	0.95144	1.24242	0.95114	0.95056	0.91838
Maximum resolution (Å)	1.45	1.6	2.0	2.0	2.0
Total reflections	158,237	303,771	264,621	513,582	317,548
Unique Reflections	28,262	19,475	18,607	19,990	19,594
Redundancy[b]	2.4 (1.8)	3.5 (2.8)	1.8 (1.4)	3.7 (2.9)	1.9 (1.6)
Completeness,[b] (%)	96.0 (64.1)	94.2 (70.1)	92.0 (61.1)	98.7 (91.1)	96.5 (78.8)
$\langle I \rangle / \langle \sigma(I)$[b]	26.4 (3.0)	34.9 (3.5)	10.3 (2.2)	19.5 (4.3)	11.25 (2.6)
R_{sym}[b,c]	0.035 (0.220)	0.043 (0.160)	0.048 (0.233)	0.051 (0.222)	0.046 (0.216)
Phasing (20.0–2.5 Å resolution range)					
Figure of merit	0.57				
Refinement Statistics					
	+ Native Peptide	+ Mutant Peptide			
R_{cryst}/R_{free}[d]	0.198/0.235	0.235/0.294			
Protein atoms/Ca^{2+}	1355/4	1348/4			
Water molecules	390	370			
Rms deviation from ideal bond (Å)/angle (°)	0.004/0.986	0.005/0.96			

[a] Crystals of both the complexes are isomorphous. They belong to the C2 space group with one molecule in the asymmetric unit. The native domain crystal has the following unit cell dimensions: a = 86.02 Å; b = 30.96 Å; c = 63.94 Å; and α = 90°; β = 114.54°; γ = 90°.
[b] Values in parenthesis are for the highest resolution shell.
[c] $R_{sym} = \Sigma_{hkl} |I_{hkl} - \langle I_{hkl} \rangle| / \Sigma_{hkl} I_{hkl}$.
[d] R factor = $\Sigma_{hkl} ||F_o| - |F_c|| / \Sigma_{hkl} |F_o|$, where $|F_o|$ and $|F_c|$ are the observed and calculated structure factor amplitudes for reflection hkl. R_{free} was calculated with a 5% subset of randomly chosen reflections not included in any stage of the refinement.

represent the conformation of the fully calcium-loaded CaM that produces CDF (i.e., fully Ca^{2+} saturated at both lobes with both lobes interacting with the IQ motif). As discussed previously, this is consistent with the finding that mutation of I1672 to alanine permits CDF, whereas mutation to glutamate abolishes CDF (Zühlke et al., 1999, 2000). From the structure above, a glutamate substitution could introduce a negative charge deep into the hydrophobic pocket of the C lobe and thereby greatly diminish the interaction of CaM with this region.

The finding that the mutation of IQ to AA does not greatly alter the conformation of CaM bound to the IQ motif (Figure 3) is also consistent with biochemical studies (Tang et al., 2003; Zühlke et al., 2000). Hence, the alanine mutations are apparently not abolishing CDI by changing the ability of CaM to interact with the IQ motif. A more likely explanation is found in the model proposed by Kim et al. (2004), in which intramolecular interactions of the isoleucine and glutamine residues themselves are necessary for transducing the signal from the Ca^{2+} sensor to the inactivation machinery. Zhang et al. (2005) have also suggested that the IQ sequence may be involved in interactions with other sequences within $Ca_V1.2$. Since the isoleucine residue is buried in our structure, it is possible that, for CDI to occur, one of the lobes of CaM must move (perhaps to engage either the A or C motifs at amino acids 1609–1628 and 1627–1652, respectively) to expose the IQ residues and allow them to interact with the sequences that couple Ca^{2+} binding to CaM inactivation. Another option is that CDI occurs when Ca^{2+} is only bound to the C lobe of CaM. A partially Ca^{2+}-saturated CaM is likely to have a very different conformation and/or to engage other binding determinants within the channel, leading to exposure of the IQ sequence. A role of a partially Ca^{2+}-saturated CaM in CDI is supported by the finding that only Ca^{2+} binding to the C lobe CaM is required for CDI (Peterson et al., 1999).

Experimental Procedures

Materials

Complex of recombinant mammalian Ca^{2+}-CaM was expressed and purified using established methods (Gopalakrishna and Anderson, 1982; Rodney et al., 2000). Synthetic peptides were produced at the protein lab facility at Baylor College of Medicine with amino acid numbering according to Swiss-Prot accession number Q13936. 1 μmol of peptide was added to 200 nmol CaM in 20 mM MOPS (pH 7.4), 10 mM $CaCl_2$. The complex was eluted from a HiLoad 16/60 Superdex 75 (Amersham Biosciences Corp, Piscataway, NJ) molecular sieving column, and concentrated to 8–10 mg/ml.

Structure Determination

Crystals of the complex were grown by vapor diffusion, with drops made by mixing 4 μl of the complex with 2 μl of the well solution (32% PEG 4000 [Fluka, Milwaukee, WI], 50 mM Tris, 50 mM $MgCl_2$ [pH 8.3]). The lead nitrate derivative of the IQ complex crystal was created by a 1 mM overnight soak. Crystals were flash-cooled at 100 K, and native and multiwavelength anolmalous dispersion (MAD) data were collected at the Gulf Coast Protein Crystallography Consortium (GCPCC) beamline at the Louisiana State University Center for Advanced Microstructures and Devices (Baton Rouge, LA). Data were reduced with the HKL2000 software package (Otwinowski and Minor, 1997), and the structure solved by MAD phasing and refined using CNS (Brünger et al., 1998) and the CHAIN graphics program (Sack and Quiocho, 1997). Similar procedures were used for the crystallization and intensity data collection of the complex with the alanine-substituted (I1672 and Q1673) mutant peptide. The crystal of the complex with the mutant peptide is isomorphous with that of the complex with the wild-type peptide. Data collection and refinement statistics are shown in Table 1.

Acknowledgments

We gratefully acknowledge data collection assistance by Dr. Henry Bellamy and David Neau at the Center for Advanced Microstructures and Devices GCPCC beamline. This work was supported by grants from the National Institutes of Health (grants AR41802 and AR44864 to S.L.H., and GM021371 to F.A.Q.), the Muscular Dystrophy Association (to S.L.H.), and the Welch Foundation (Q-0581 to F.A.Q).

Received: August 3, 2005
Revised: September 29, 2005
Accepted: September 30, 2005
Published: December 13, 2005

References

Alseikhan, B.A., DeMaria, C.D., Colecraft, H.M., and Yue, D.T. (2002). Engineered calmodulins reveal the unexpected eminence of Ca^{2+} channel inactivation in controlling heart excitation. Proc. Natl. Acad. Sci. USA *99*, 17185–17190.

Babu, Y.S., Sack, J.S., Greenhough, T.J., Bugg, C.E., Means, A.R., and Cook, W.J. (1985). Three-dimensional structure of calmodulin. Nature *315*, 37–40.

Bhattacharya, S., Bunick, C.G., and Chazin, W.J. (2004). Target selectivity in EF-hand calcium binding protein. Biochim. Biophys. Acta *1742*, 69–79.

Black, D.J., Halling, D.B., Mandich, D.V., Pedersen, S.E., Altschuld, R.A., and Hamilton, S.L. (2005). Calmodulin interactions with IQ peptides from voltage-dependent calcium channels. Am. J. Physiol. Cell Physiol. *288*, C669–C676.

Bourinet, E., Charnet, P., Tomlinson, W.J., Stea, A., Snutch, T.P., and Nargeot, J. (1994). Voltage-dependent facilitation of a neuronal alpha 1C L-type calcium channel. EMBO J. *13*, 5032–5039.

Brünger, A.T., Adams, P.D., Clore, G.M., DeLano, W.L., Gros, P., Grosse-Kunstleve, R.W., Jiang, J.S., Kuszewski, J., Nilges, M., Pannu, N.S., et al. (1998). Crystallography & NMR system: a new software suite for macromolecular structure determination. Acta Crystallogr. D Biol. Crystallogr. *54*, 905–921.

Dascal, N., Snutch, T.P., Lubbert, H., Davidson, N., and Lester, H.A. (1986). Expression and modulation of voltage-gated calcium channels after RNA injection in *Xenopus* oocytes. Science *231*, 1147–1150.

Drum, C.L., Yan, S.-Z., Bard, J., Shen, Y.-Q., Lu, D., Soelaiman, S., Grabarek, Z., Bohm, A., and Tang, W.-J. (2002). Structural basis for the activation of anthrax adenylyl cyclase exotoxin by calmodulin. Nature *415*, 396–402.

Erickson, M.G., Liang, H., Mori, M.X., and Yue, D.T. (2003). FRET two-hybrid mapping reveals function and location of L-type Ca^{2+} channel CaM preassociation. Neuron *39*, 97–107.

Fallon, J.L., and Quiocho, F.A. (2003). A closed compact structure of native Ca^{2+}-calmodulin. Structure *11*, 1303–1307.

Gopalakrishna, R., and Anderson, W.B. (1982). Ca^{2+}-induced hydrophobic site on calmodulin: application for purification of calmodulin by phenyl-Sepharose affinity chromatography. Biochem. Biophys. Res. Commun. *104*, 830–836.

Imredy, J.P., and Yue, D.T. (1994). Mechanism of Ca^{2+}-sensitive inactivation of L-type Ca^{2+} channels. Neuron *12*, 1301–1318.

Kim, J., Ghosh, S., Nunziato, D.A., and Pitt, G.S. (2004). Identification of the components controlling inactivation of voltage-gated Ca^{2+} channels. Neuron *41*, 745–754.

Kobrinsky, E., Tiwari, S., Maltsev, V.A., Harry, J.B., Lakatta, E., Abernethy, D.R., and Soldatov, N.M. (2005). Differential role of the alpha1C subunit tails in regulation of the Cav1.2 channel by membrane potential, beta subunits, and Ca^{2+} ions. J. Biol. Chem. *280*, 12474–12485.

Lehmann-Horn, F., and Jurkat-Rott, K. (1999). Voltage-gated ion channels and hereditary disease. Physiol. Rev. *79*, 1317–1372.

Lim, N.F., Nowycky, M.C., and Bookman, R.J. (1990). Direct measurement of exocytosis and calcium currents in single vertebrate nerve terminals. Nature *344*, 449–451.

Lipscombe, D., Helton, T.D., and Xu, W. (2004). L-type calcium channels: the low down. J. Neurophysiol. *92*, 2633–2641.

Meador, W.E., Means, A.R., and Quiocho, F.A. (1992). Target enzyme recognition by calmodulin: 2.4 Å structure of a calmodulin-peptide complex. Science *257*, 1251–1255.

Meador, W.E., Means, A.R., and Quiocho, F.A. (1993). Modulation of calmodulin plasticity in molecular recognition on the basis of X-ray structures. Science *262*, 1718–1721.

Meador, W.E., George, S.E., Means, A.R., and Quiocho, F.A. (1995). X-ray analysis reveals conformational adaptation of the linker in functional calmodulin mutants. Nat. Struct. Biol. *2*, 943–945.

Mori, M.X., Erickson, M.G., and Yue, D.T. (2004). Functional stoichiometry and local enrichment of calmodulin interacting with Ca^{2+} channels. Science *304*, 432–435.

Osawa, M., Tokumitsu, H., Swindells, M.B., Kurihara, H., Orita, M., Shibanuma, T., Furuya, T., and Ikura, M. (1999). A novel target recognition revealed by calmodulin in complex with Ca^{2+}-calmodulin-dependent kinase kinase. Nat. Struct. Biol. *6*, 819–824.

Otwinowski, Z., and Minor, W. (1997). Processing of X-ray diffraction data collected in oscillation mode. Meth. Enzymol. *276*, 307–326.

Pate, P., Mochca-Morales, J., Wu, Y., Zhang, J.Z., Rodney, G.G., Serysheva, I.I., Williams, B.Y., Anderson, M.E., and Hamilton, S.L. (2000). Determinants for calmodulin binding on voltage-dependent Ca^{2+} channels. J. Biol. Chem. *275*, 39786–39792.

Peterson, B.Z., DeMaria, C.D., Adelman, J.P., and Yue, D.T. (1999). Calmodulin is the Ca^{2+} sensor for Ca^{2+}-dependent inactivation of L-type calcium channels. Neuron *22*, 549–558.

Pitt, G.S., Zuhlke, R.D., Hudmon, A., Schulman, H., Reuter, H., and Tsien, R.W. (2001). Molecular Basis of Calmodulin Tethering and Ca^{2+}-dependent Inactivation of L-type Ca^{2+} Channels. J. Biol. Chem. *276*, 30794–30802.

Rodney, G.G., Williams, B.Y., Strasburg, G.M., Beckingham, K., and Hamilton, S.L. (2000). Regulation of RYR1 activity by Ca^{2+} and calmodulin. Biochemistry *39*, 7807–7812.

Romanin, C., Gamsjaeger, R., Kahr, H., Schaufler, D., Carlson, O., Abernethy, D.R., and Soldatov, N.M. (2000). Ca^{2+} sensors of L-type Ca^{2+} channel. FEBS Lett. *487*, 301–306.

Sack, J.S., and Quiocho, F.A. (1997). CHAIN-A crystallographic modeling program. Meth. Enzymol. *277*, 158–173.

Schumacher, M.A., Rivard, A.F., Bachinger, H.P., and Adelman, J.P. (2001). Structure of the gating domain of a Ca^{2+}-activated K^+ channel complexed with Ca^{2+}calmodulin. Nature *410*, 1120–1124.

Tang, W., Sencer, S., and Hamilton, S.L. (2002). Calmodulin modulation of proteins involved in excitation-contraction coupling. Front. Biosci. *7*, d1583–d1589.

Tang, W., Halling, D.B., Black, D.J., Pate, P., Zhang, J.Z., Pedersen, S., Altschuld, R.A., and Hamilton, S.L. (2003). Apocalmodulin and Ca^{2+} calmodulin-binding sites on the CaV1.2 channel. Biophys. J. *85*, 1538–1547.

Zhang, R., Dzhura, I., Grueter, C.E., Thiel, W., Colbran, R.J., and Anderson, M.E. (2005). A dynamic alpha-beta inter-subunit agonist signaling complex is a novel feedback mechanism for regulating L-type Ca2+ channel opening. FASEB J. *19*, 1573–1575.

Zühlke, R.D., Pitt, G.S., Deisseroth, K., Tsien, R.W., and Reuter, H. (1999). Calmodulin supports both inactivation and facilitation of L-type calcium channels. Nature *399*, 159–162.

Zühlke, R.D., Pitt, G.S., Tsien, R.W., and Reuter, H. (2000). Ca^{2+}-sensitive inactivation and facilitation of L-type Ca^{2+} channels both depend on specific amino acid residues in a consensus calmodulin-binding motif in the (alpha)1C subunit. J. Biol. Chem. *275*, 21121–21129.

Accession Numbers

Two sets of coordinates have been deposited in the Protein Data Bank with accession codes 2F3Y and 2F3Z.